Surfaces and Interfaces 25 (2021) 101268

Contents lists available at ScienceDirect

Surfaces and Interfaces

journal homepage: www.sciencedirect.com/journal/surfaces-and-interfaces

Development of a novel methyl germanane modified disposable sensor and its application for voltammetric phenol detection

Gulsah Congur [a,b,*]

[a] Bilecik Seyh Edebali University, Vocational School of Health Services, 11230 Bilecik, Turkey
[b] Bilecik Seyh Edebali University, Biotechnology Application and Research Center, 11230, Bilecik, Turkey

ARTICLE INFO

Keywords:
Methyl germanane
Pencil graphite electrode
Phenol
cyclic voltammetry

ABSTRACT

Germanane is a novel 2D material and a good candidate for electrochemical applications due to it has high electron mobility and direct band gap. Methyl germanane (m-GMN) is a covalently terminated germanane and has superior catalytic activity, electron mobility and stability. Herein, m-GMN modified chemically activated pencil graphite electrodes (m-GMN/c-PGEs) were developed and m-GMN/c-PGEs were utilized for voltammetric detection of phenol (PNL). Chemical activation of PGEs (c-PGEs) was firstly performed, then m-GMN was modified at the surface of c-PGEs. Electrochemical and microscopic characterizations of m-GMN/c-PGEs were performed. The detection limits (LODs) were estimated as 0.72 μg/mL (7.65 μM) and 0.35 μg/mL (3.72 μM) using c-PGEs and m-GMN/c-PGEs, respectively. Application of the sensor was tested in water samples and the selectivity of the sensor system was tested against Cu^{2+}, Hg^{2+}, 2,4-dichlorophenoxyacetic acid, 2,6-di-tert-butyl-4-methylphenol, D(+)glucose and paracetamol. A novel electrochemical sensor which had crucial properties such as being reproducible, repeatable, and stable was developed for PNL detection by the development of m-GMN/c-PGEs.

1. Introduction

Discovery of graphene started to a new era into material science by introducing the concept of 'two-dimensional (2D) materials'. 2D materials have unique properties [1–3] including high electrical conductivity. Therefore, application of 2D materials into the electrochemical (bio) sensor area is an attractive topic. They enhance electron mobility at the electrode/electrolyte interface and provide high surface area by modification of them onto the (bio)sensor surface which resulted to reach low detection limits.

Among other 2D materials, germanane (GMN) is a novel 2D material synthesized as honeycomb-like sp^3-hybridized network layer structure of germanium atoms [4]. It is a promising material for electronics and optoelectronics [5,6], energy storage and conversion [7]. Its applications into (bio)sensing area were shown by different research groups [8,9]. Srimathi and coworkers developed a nanosensor using GMN nanosheets for detection of liver cirrhosis biomarkers [8] which were volatile organic compounds (VOCs). The binding mechanisms of the VOCs onto GMN nanosheet were evaluated and found that methanol binding was less and binding of limonene was the most effective. Adsorption of DNA and RNA molecules onto GMN nanosheet was also investigated by the same research group [9]. They found the order of the adsorption of nucleobases as Cytosine>Guanine>Adenine>Tyhmine>Uracil. They concluded that GMN nanosheet provided an immobilization surface for nucleobases and GMN has a potential for further nanobiosensor designs.

It has been reported that covalent surface termination can be a powerful method for the controlled tuning of material properties [10]. Recent studies showed that covalently-terminated GMN has systematic optoelectronic [11] and catalytic properties [12]. Jiang and coworkers [10] reported that methyl termination of GMN enhanced its thermal stability from 75 °C to 250 °C and increased the band gap by ~0.1 to 1.7 eV which indicates enhanced electronic properties can be achieved by methyl termination of GMN.

Development of monitoring systems that are sensitive, practical, affordable, reliable, fast and miniaturized analytical tools is an attractive topic in today's world struggling with pandemic diseases and environmental hazards [13–16]. Electrochemical biosensor designs possess the crucial properties listed above. Moreover, surface modification of countless number of nanomaterials/biomaterials or their nanobiocomposites can be investigated by using electrochemical techniques [17–22]. The combination of advanced nanotechnological approaches and electrochemical biosensing strategies provides

* Corresponding author.
E-mail address: gulsah.congur@bilecik.edu.tr.

https://doi.org/10.1016/j.surfin.2021.101268
Received 8 April 2021; Received in revised form 26 May 2021; Accepted 2 June 2021
Available online 10 June 2021

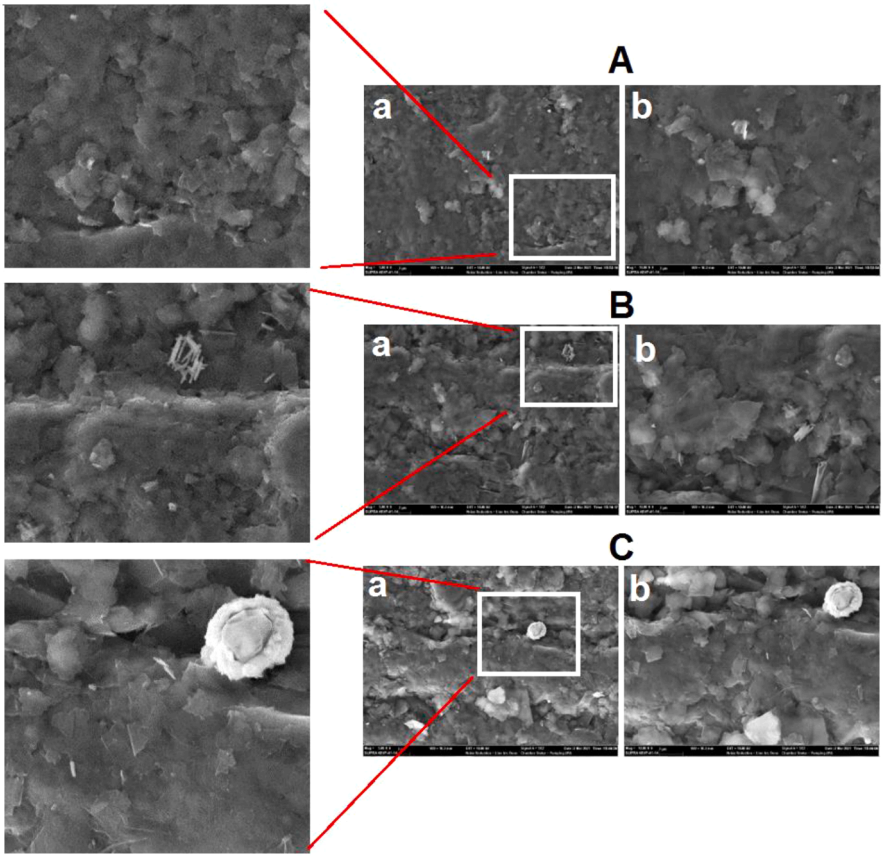

Fig. 1. SEM images of PGE **(A)** c-PGE **(B)** and 2000 μg/mL m-GMN modified c-PGE **(C).** The acceleration voltage was 10.0 kV, the resolutions were 5000x **(a)** and 10000x **(b)**.

development of not only sensitive but also selective and miniaturized lab-on-a chip technologies. Therefore, the electrochemical nano-biosensor area has been growing day-by-day.

Pencil graphite electrodes (PGEs) allow to design robust, sensitive and selective electrochemical (bio)sensor platforms [23–27]. PGE based electrochemical biosensor systems are practical and time-saver analysis platforms since they could be prepared without polishing, grinding, filling or sonication steps compared to other carbon electrodes [28,29]. The graphite leads can be purchased from local markets. Due to their disposable structure, they do not require to implement extra washing and cleaning steps for reuse. Therefore, they are practical, time-saver, eco-friendly, affordable and accessible and these unique properties make them a good candidate for development of prototypes for future hand-held and miniaturized devices [30,31].

Herein, a methyl germanane (m-GMN) modified disposable biosensor was developed and its application was tested for detection of phenol (PNL) since PNL and its derivatives are the raw materials for pharmaceuticals [32], pesticides [33], plastics [34] and petrochemicals [35]. PNL is a water contaminant as a result of industrialization [36]. First, chemical activation of the PGEs were performed, then m-GMN was modified onto chemically activated PGEs (c-PGEs). The experimental conditions were optimized, m-GMN modification was characterized using microscopic and electrochemical techniques. The electrochemical detection of PNL was done by c-PGEs and m-GMN/c-PGEs and the detection of PNL was tested in different water samples. The selectivity of the sensor was also investigated using metal ions or other organic compounds. Until today, there is no report in the literature for the development of m-GMN modified PGEs by chemical activation process and electrochemical monitoring of PNL using m-GMN/c-PGEs.

2. Materials and methods

2.1. Apparatus

For each electrochemical measurement, IVIUM Compactstat.e with IVIUM Release 4.951 software package (Holland) was used as the potentiostat.

Three electrode system was used for all electrochemical measurements. Graphite leads were used for the fabrication of pencil graphite electrodes (PGEs). The leads were obtained from local market. The electrochemical cell composed of a working electrode as PGE, a reference electrode as Ag/AgCl/3 M KCl (BAS, Model RE-5B, W. Lafayette, USA) and an auxiliary electrode as a platinum wire. 14 mm of the graphite lead was vertically holded by a pencil (Rotring, Germany) and 10 mm of each lead was immersed into the activation/modification/measurement solutions. The electrical contact of the pencil was done by soldering a metallic wire to the metallic part.

2.2. Chemicals

Methyl germanane (m-GMN), dimethyl sulfoxide (DMSO), phenol (PNL), $CuSO_4$, $HgCl_2$, 2,4-dichlorophenoxyacetic acid (2,4-D), 2,6-di-tert-butyl-4-methylphenol (m-PNL), D(+)glucose, potassiumhexacyanoferrate(III) ($K_3Fe(CN)_6$), potassiumhexacyanoferrate(II) trihydrate ($K_4Fe(CN)_6 \bullet 3H_2O$) and potassium chloride (KCl) were purchased from Sigma-Aldrich. Paracetamol (PRL) was purchased from drugstore and their stock concentrations were 10000 μg/mL and 25000 μg/mL, respectively. The stock solutions of PNL, D(+)glucose, $CuSO_4$ and $HgCl_2$ were prepared with 50 mM phosphate buffer solution (PBS; pH 7.40) as 1000 μg/mL. The stock solutions of 2,4-D and m-PNL were prepared in DMSO as 1000 μg/mL. Diluted solutions of all interference factors were

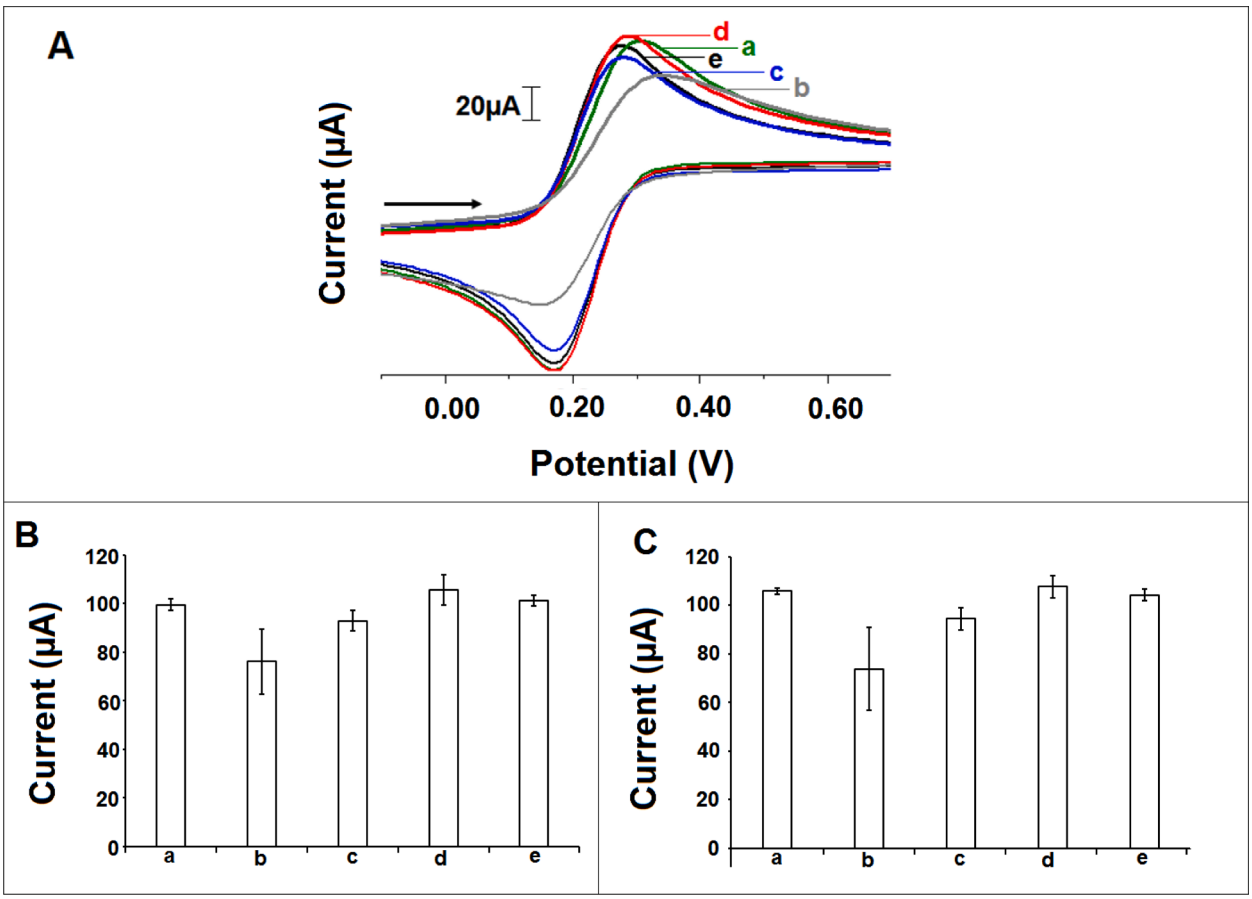

Fig. 2. Cyclic voltammograms **(A)** or histograms representing the average anodic current (I_a) **(B)** and cathodic currrent (I_c) **(C)** values of PGEs **(a),** c-PGEs **(b),** 1000 **(c),** 2000 **(d)** and 3000 **(e)** μg/mL m-GMN modified c-PGEs ($n = 3$). CV measurements were done in the anionic redox probe contained 2 mM $K_3[Fe(CN)_6]/K_4[Fe(CN)_6]$ (1:1) in 0.10 M KCl.

prepared in PBS (pH 7.40).

All analytical reagent grade chemicals supplied from Sigma-Aldrich and Merck were used for all experiments. All buffers were prepared in Milli-Q water.

2.3. Procedure

2.3.1. Preparation of m-GMN solution

1000-3000 μg/mL m-GMN was dissolved in DMSO by sonication during 30 min.

2.3.2. Chemical activation of disposable PGEs

Each PGE was immersed into 100 μL of 1 M NaOH sample during 1 h. Then, the electrodes were immersed into ultrapure water during 5 s to eliminate unspecific formation at the graphite surface.

2.3.3. Preparation of m-GMN modified c-PGEs

The chemically activated PGEs (c-PGEs) were dipped into the vials containing 40 μL of 1000–3000 μg/mL m-GMN during 15 min at dark. Then, the modified electrodes dried upward position during 5 min.

2.3.4. Detection of PNL

The three electrode system was immersed into 2 mL of 1–5 μg/mL PNL sample prepared in PBS (pH 7.40) [37], then cyclic voltammetry (CV) measurements were performed [38,39]. The potential range was from +0.30 V to +0.90 V at the scan rate as 50 mV/s. For real sample analysis, stock solution of PNL was spiked into 2 mL of tap water, drinking water or industrial waste water samples. Tap water and drinking water samples were boiled during 10 min and stored at room temperature during 36 h for precipitation of chlorinated molecules. Upper part of the tap water or drinking water samples were used for the electrochemical analysis.

2.3.5. Electrochemical characterization

2.3.5.1. Voltammetric measurements. For optimization of m-GMN concentration and the electrochemical characterization studies, CV technique was applied. Measurements were performed in an anionic redox probe consisted of 2.00 mM $K_3[Fe(CN)_6]/K_4[Fe(CN)_6]$ (1:1) prepared in 0.10 M KCl as supporting electrolyte. The potential range was from −0.45 V to +1.20 V at the scan rate as 50 mV/s. Anodic and cathodic peak current values (I_a and I_c, respectively) was measured to monitor the chemical activation of PGEs and the modification of m-GMN at c-PGE surface. Anodic and cathodic charge (Q_a and Q_c, respectively) and I_a and I_c, values were measured at the same time.

2.3.5.2. Impedimetric measurements. Electrochemical impedance spectroscopy (EIS) technique was used for impedimetric measurements. An anionic redox probe containing 2.50 mM $K_3[Fe(CN)_6]/K_4[Fe(CN)_6]$ (1:1) prepared in 0.10 M KCl was used for all measurements. The frequency range was from 100 mHz to 100 kHz at an AC potential of with a sinusoidal signal of peak-to-peak amplitude as 10 mV. The frequency interval divided into 98 logarithmically equidistant measure points. Randles circuit was selected as the equivalent circuit model for fitting all impedance data. R_{ct}, R_s, Q and W represent the respective semicircle diameter corresponds to the charge-transfer resistance, the solutions resistance, the capacitance, and Warburg impedance, respectively.

All experimental steps were done at room temperature.

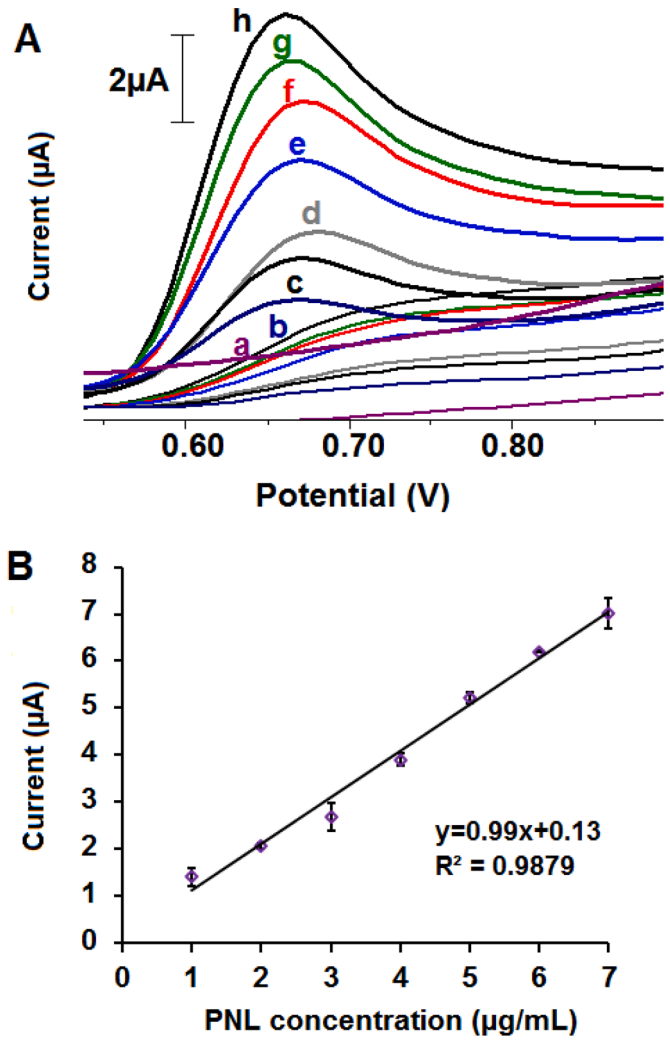

Fig. 3. Voltammograms **(A)** of c-PGE **(a),** 1 (b), 2 **(c),** 3 **(d)**, 4 **(e),** 5 **(f),** 6 **(g)** and 7 **(h)** μg/mL PNL measured by c-PGEs. Line graph was drawn **(B)** based on the average PNL signals of 1–7 μg/mL PNL obtained by using c-PGEs (n = 3).

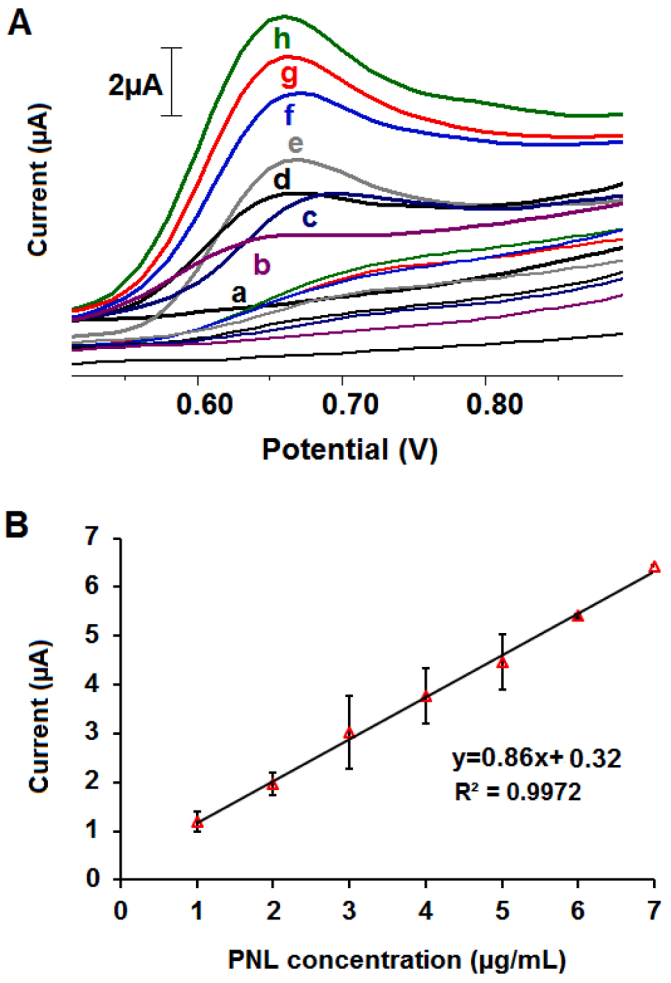

Fig. 4. Voltammograms **(A)** of GMN/c-PGE **(a),** 1 (b), 2 **(c),** 3 **(d)**, 4 **(e),** 5 **(f),** 6 **(g)** and 7 **(h)** μg/mL PNL measured by GMN/c-PGEs. Line graph was drawn **(B)** based on the average PNL signals of 1–7 μg/mL PNL obtained by using m-GMN/c-PGEs (n = 3).

3. Results and discussion

3.1. m-GMN modification of PGEs

The microscopic characterization of chemical activation of PGEs and m-GMN modification of c-PGEs were studied and the results were shown in Fig. 1. Layered graphite surface of PGEs was visualized in Fig. 1A and morphological change at the graphite surface by chemical activation was clearly shown in Fig. 1B, especially zoomed picture of the one obtained using 5000x resolution (Fig. 1B-a). 2000 μg/mL m-GMN modification resulted the coverage of the layered surface of c-PGEs by obtaining smooth area (Fig. 1C-a and b) and partial coverage was monitored and given in the zoomed picture.

The elemental concentrations of oxygen, carbon, sodium and germanium atoms obtained by Energy dispersive X-ray spectroscopy (EDX) were given in Table S1. Weight% of oxygen and sodium ions increased after chemical activation (Table S1-A to B) and weight% of germanium ions increased from zero to 2.62 after m-GMN modification (Table S1-B to C). These results indicated that m-GMN modification at the surface of c-PGEs was succesfully achieved.

The effect of m-GMN concentration upon the sensor response was investigated. First, chemical activation of PGEs was performed, then m-GMN at different concentration level from 1000 to 3000 μg/mL was modified at the surface of c-PGE. CV measurements were done in the anionic redox probe and the changes at the anodic and cathodic peak currents (I_a and I_c, respectively) were represented in Fig. 2. After chemical activation of PGE, the I_a and I_c values decreased (Fig. 2A-a to b). This decrease may be attributed that the chemical activation resulted formation of carboxyl groups [40] which caused repulsive interactions between anionic redox probe and negatively charged electrode surface [41]. m-GMN modification of the c-PGEs resulted the increase I_a and I_c values (Fig. 2A-b to c-e). The peak to peak separation (ΔE_p) values of PGEs, c-PGEs and m-GMN modified PGEs were found to be 130 mV, 230 mV and 100 mV, respectively. These results indicated that the electrochemical reaction of $K_3[Fe(CN)_6]$ and $K_4[Fe(CN)_6]$ ions onto c-PGEs was irreversible whereas m-GMN modification made the reaction quasi-reversible due to the fact that m-GMN decreased charge transfer resistance occurred electrode/electrolyte interface [42]. The increase at the I_a and I_c values and the changes at the ΔE_p value were in an agreement with the results reported by Rosli et al [43] who studied the modification of glassy carbon electrode (GCE) with siloxene, germanane and methyl germanane. m-GMN modification was successfully achieved by formation of covalent bindings between carboxyl groups of PGEs and methyl groups of m-GMNs. m-GMN provided low charge transfer resistance [42] at the electrode/electrolyte interface and I_a and I_c values increased. After three repetitive measurements, the average I_a and I_c values was found to be 99.45 ± 2.47 μA (Fig. 2B-a) and 105.85 ± 1.20 μA (Fig. 2C-a) by using PGEs (relative standard deviation% (RSD%) = 2.48% and 1.1%, respectively). After chemical activation of the PGEs,

Table 1
Reports for development of electrochemical sensors for detection of PNL and its derivatives. **Abbreviations: 2,4,6-TCP:** 2,4,6-trichlorophenol, **CC:** Cathecol, **PN, P, PNL:** Phenol, ***p*-NP:** *p*-nitrophenol, **BPA:** Bisphenol A, **4-NP:** 4-nitrophenol, **4PP:** 4-phenoxyphenol, **4MP:** 4-methoxyphenol, **2-CP:** 2-chlorophenol, **4-CP:** 4-chlorophenol, **2,4-CP:** 2,4-dichlorophenol **AgNPs-PDA-GR/GCE:** Ag nanoparticles polydopamine-reduced graphene oxide modified glassy carbon electrode, **CoPcNRs/FA-rGO/GCE:** Fulvic acid reduced graphene oxide and and Co-phthalocyanine nanorods modified GCE, **PANI-GO/GCE:** Partially-reduced-GO-sheet-covered polyaniline nanotubes modified GCE, **Mn-Fe_3O_4/3D-G/GCE:** N-doped three-dimensional graphene (3D-G) with Mn-doped Fe_3O_4 nanoparticles modified GCE, **CPE:** Carbon paste electrode, **Au NPs/CNTs electrode:** Au nanoparticles decorated carbon nanotubes electrode, **BDDE:** Boron-doped diamond electrode, **NiZn-MOF NSs/GCE:** 2D bimetallic metal organic framework nanosheets modified GCE, **NPG:** Nanoporous gold, **DPV:** Differential pulse voltammetry, **SWV:** Square wave voltammetry.

Analyte	Type of (bio)sensor	Analysis method	Limit of detection	Preparation time	Application in real sample	Reference
PNL	Au NPs/CNTs electrode	DPV	6nM	N.R.	Industrial wastewater	[37]
2,4,6-TCP	AgNPs-PDA-GR/GCE	DPV	0.7nM	~31h	Lake water	[49]
CC, PN, *p*-NP	CoPcNRs/FA-rGO/GCE	DPV	0.3μM, 0.65μM, 0.65μM	~26h	River water	[50]
BPA and PN	PANI-GO/GCE	CV	0.5nM and 4.5nM	~49h	Drinking water	[51]
4-NP	Mn-Fe_3O_4/3D-G/GCE	CV	19nM	~30h	Tap water, river water, domestic sawage	[52]
4PP, 4MP, P	CPE	SWV	2.5μM, 2.5μM and 5μM	N.R.	N.R.	[53]
PNL, 2-CP 4-CP 2,4-CP	BDDE	CV	500 μg/L, 300 μg/L, 750 μg/L, 1000μg/L	N.R.	Drinking water	[54]
PNL	NiZn-MOF NSs/GCE	Amperometry	6.5nM	~17h	Tap water	[55]
PNL,CC	NPG thin film	Amperometry	0.5μM in PBS (pH 7.2), 0.1μM in 0.1 M H_2SO_4	N.R.	N.R.	[56]
PNL	m-GMN/c-PGE	CV	0.35μg/mL (3.72μM)	1h 45 min	Tap water, drinking water, waste water	This study

* *N.R.:Not Reported.*

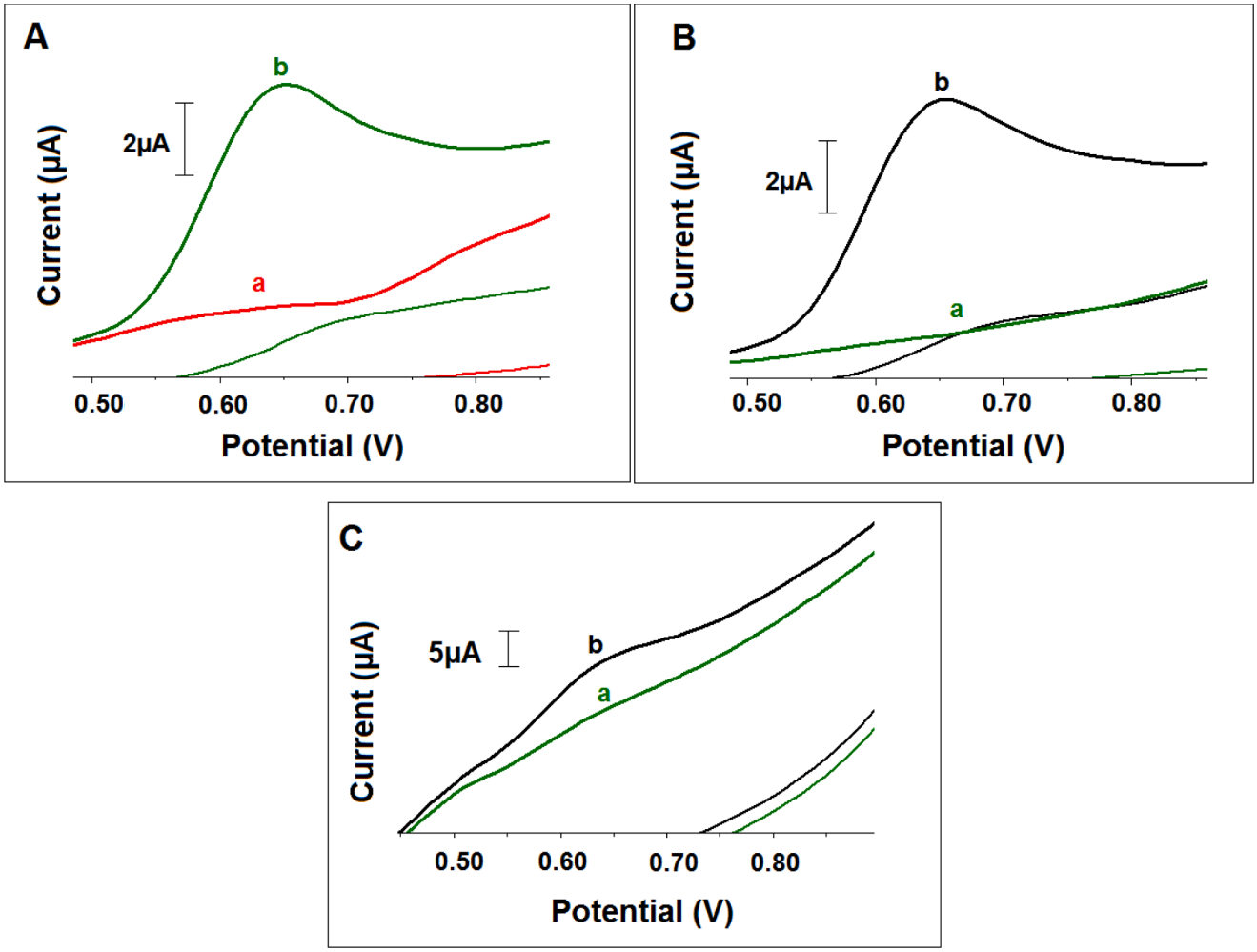

Fig. 5. Voltammograms of tap water **(a)** and 5 μg/mL PNL in tap water **(b) (A).** Voltammograms of drinking water **(a)** and 5 μg/mL PNL in drinking water **(b) (B).** Voltammograms of industrial waste water **(a)** and 5 μg/mL PNL in of industrial waste water **(b) (C).**

Table 2
The average signals ($n = 3$) of 5 μg/mL PNL in tap water, drinking water or industrial waste water and control signals of drinking water or industrial waste water.

	PNL signal	Control signal	Recovery %
Tap water	4.66 μA (RSD%= 2.93%)	0.26 μA (RSD%= 4.04%)	101.17%
Drinking water	4.51 μA (RSD%= 8.84%)	0	97.55%
Industrial waste water	4.13 μA (RSD%= 3.67%)	0.76 μA (RSD%= 16.37%)	93.00

the average I_a and I_c values were measured as 76.07 ± 13.48 μA and 73.75 ± 17.05 μA with the RSDs% as 17.73% and 23.10%, respectively ($n = 3$) and the decrease ratios of the average I_a and I_c values were calculated as 23.51% and 30.31%. The highest increase at the average I_a and I_c values could be obtained after 2000 μg/mL m-GMN modification (Fig. 2B-b to d and 2C-b to d) and increase ratios were found to be 38.66% and 41.33%, respectively. m-GMN modification was successfully performed by obtaining reproducible I_a and I_c values, the RSD% values were found to be 5.91% and 4.30% respectively after 2000 μg/mL m-GMN modification at the c-PGE surface. The anodic (Q_a) and cathodic (Q_c) charge values of PGE, c-PGE and 2000 μg/mL m-GMN modified c-PGE were represented in Table S2. The changes at the Q_a and Q_c values were in parallel with the ones obtained by I_a and I_c values. Based on the CV results, 2000 μg/mL m-GMN concentration level was determined as optimum for further studies.

Effective surface area (A_{eff}) values of PGE, c-PGE and 2000 μg/mL modified m-GMN/c-PGE were calculated according to the Randles–Sevcik Eq. (Eq. 1) [44–47]. The transferred electron number is n, D is the diffusion coefficient of $K_3[Fe(CN)_6]$ (7.6×10^{-6} cm^2 s^{-1}), C is the concentration of $K_3[Fe(CN)_6]$ in this equation.

$$i_p = 2.69\ 10^5 n^{3/2} A_{eff} D^{1/2}\ C\ v^{1/2} \quad (1)$$

The A_{eff} values of PGE, c-PGE and 2000 μg/mL modified m-GMN/c-PGE were calculated as 0.298, 0.222 and 0.314 cm^2, respectively. Increased A_{eff} value was obtained after m-GMN modification of c-PGE due to the fact that m-GMN modification of c-PGEs provided high surface area [42].

The electrochemical characterization of m-GMN modification was performed by EIS technique and the results were given in Figure S1. The charge transfer resistance value (R_{ct}) decreased by modification of 2000 μg/mL m-GMN at the surface of c-PGE (Fig. S1A-a to b) due to the fact that the charge transfer resistance at the electrode/electrolyte surface decreased [42] by introducing m-GMN molecules at the graphite surface. The average R_{ct} values of c-PGEs and 2000 μg/mL m-GMN modified PGEs were found to be 74±18 Ohm and 38.7±0.6 Ohm with the RSD% values as 24.05% and 1.49%, respectively. The EIS data of the other elements of equivalent circuit were given in Table S3. The impedimetric results were consistent with the voltammetric results in terms of m-GMN modification of c-PGEs. Moreover, electrochemical characterization results were in a good agreement with the microscopic results. It was concluded that m-GMN modification of c-PGEs was succesfully achieved.

3.2. Voltammetric PNL detection by using c-PGEs and m-GMN/c-PGEs

In the next step of the study, PNL detection was studied by using c-PGEs (Fig. 3) and m-GMN/c-PGEs (Fig. 4). The oxidation signal of PNL in PBS (pH 7.40) was measured at +0.66 V. The PNL signal measured by c-PGEs (Fig. 3A) or m-GMN/c-PGEs (Fig. 4A) increased while PNL concentration increased. Linear calibration graphs could be obtained at 1–7 μg/mL concentration level of PNL. The detection limits (LODs) were estimated according to the method described by Miller and Miller [48] and found to be 0.72 μg/mL (7.65 μM) and 0.35 μg/mL (3.72 μM) with the equations as $y = 0.99x+0.13$ ($R^2 = 0.9879$) and $y = 0.86x+0.32$ ($R^2 = 0.9972$) by using c-PGEs and m-GMN/c-PGEs, respectively. Large surface area for adsorption of PNL molecules was obtained by m-GMN modification of c-PGEs, therefore low LOD value could be estimated by using m-GMN/c-PGEs. The sensitivity values were calculated as 3.24 μA mL/μg cm^2 and 1.11 μA mL/μg cm^2 for c-PGEs and m-GMN/c-PGEs, respectively.

Electrochemical detection of PNL and its derivatives have been widely investigated in the literature and some of them were summarized in Table 1 [37,49–56]. Glassy carbon electrode (GCE) was used in most of the studies which required polishing and sonication treatments. Also, GCE and the other electrodes used in these studies as carbon paste electrode (CPE) and boron-doped diamond electrode (BDDE) are not single-use which means that the pretreatment steps should be done for each repetition. Although lower detection limits were estimated in some of these studies, most of them required long preparation time. As an example, Wang et al. [49] developed an electrochemical sensor system for detection of 2,4,6-trichlorophenol. They used a glassy carbon electrode (GCE) which required polishing and sonication treatments. The GCE electrode was then modified with a nanocomposite (Ag nanoparticles polydopamine-reduced graphene oxide (AgNPs-PDA-GR)) to obtain sensitive results and a moleculary imprinted polymer (MIP) was constructed onto this nanocomposite modified GCE surface. The construction of the MIP required electrochemical polymerization step, applying extra washing steps using methanol and water and removing the template molecule. The preparation of the nanocomposite and MIP system required using intensive chemical agents and implementing exhausting experimental steps whose total duration was approximately 31 h. After then, 2,4,6-TCP was monitored using differential pulse voltammetry (DPV) technique. The application of the sensor system was shown in lake water, however the fabrication of the sensor system was labor intensive and brought about environmental burden using extra chemical agents during experimental steps. In another study reported by Zhu et al. [51], partially-reduced-GO-sheet-covered polyaniline nanotubes modified GCE (PANI-GO/GCE) was developed whose total fabrication time was approximately 49 h. The developed electrode was used for detection of bisphenol A (BPA) and phenol (PN) using CV technique. The application of the sensor system was tested in drinking water, however an extraction technique should have been applied. An enzymatic biosensor was developed for detection of PNL [55] which was required approximately 17 h preparation time. The application of the biosensor was shown in tap water by filtration of the water sample. The m-GMN/c-PGE based voltammetric sensor system could detect the target molecule, PNL without long preparation time, total fabrication of the sensor required 1 h 45 min and the measurement was done in just 30 s. The m-GMN/c-PGEs were disposable, their preparation did not require to perform complex experimental procedures using intensive chemical agents. The activation or modification of the PGEs was achieved by dipping the electrodes in 100 μL or 40 μL of the sample. Therefore, the use of m-GMN/c-PGEs for detection of a contaminant factor which is monitored in water samples possesses environmental benefits in comparison to other (bio)sensor systems. Sensitive detection of PNL was achieved by using the m-GMN/c-PGEs in comparison to c-PGEs. The m-GMN/c-PGEs were time-saver, labor-friendly, practical-to-use and allowed to detect PNL sensitively. The LOD value obtained by the m-GMN/c-PGEs was quite lower than the one reported as the maximum tolerated amount of PNL as 1 mg/L in drinking water [57]. The m-GMN/c-PGE based non-enzymatic sensor system is applicable in field researches since it detected PNL in different water samples.

3.3. Real sample analysis

The applicability of the developed single-use sensor system was tested by performing voltammetric PNL detection into tap water (Fig. 5-A), drinking water (Fig. 5-B) and industrial waste water (Fig. 5-C). The detection of PNL into water samples was studied in the presence of 5 μg/

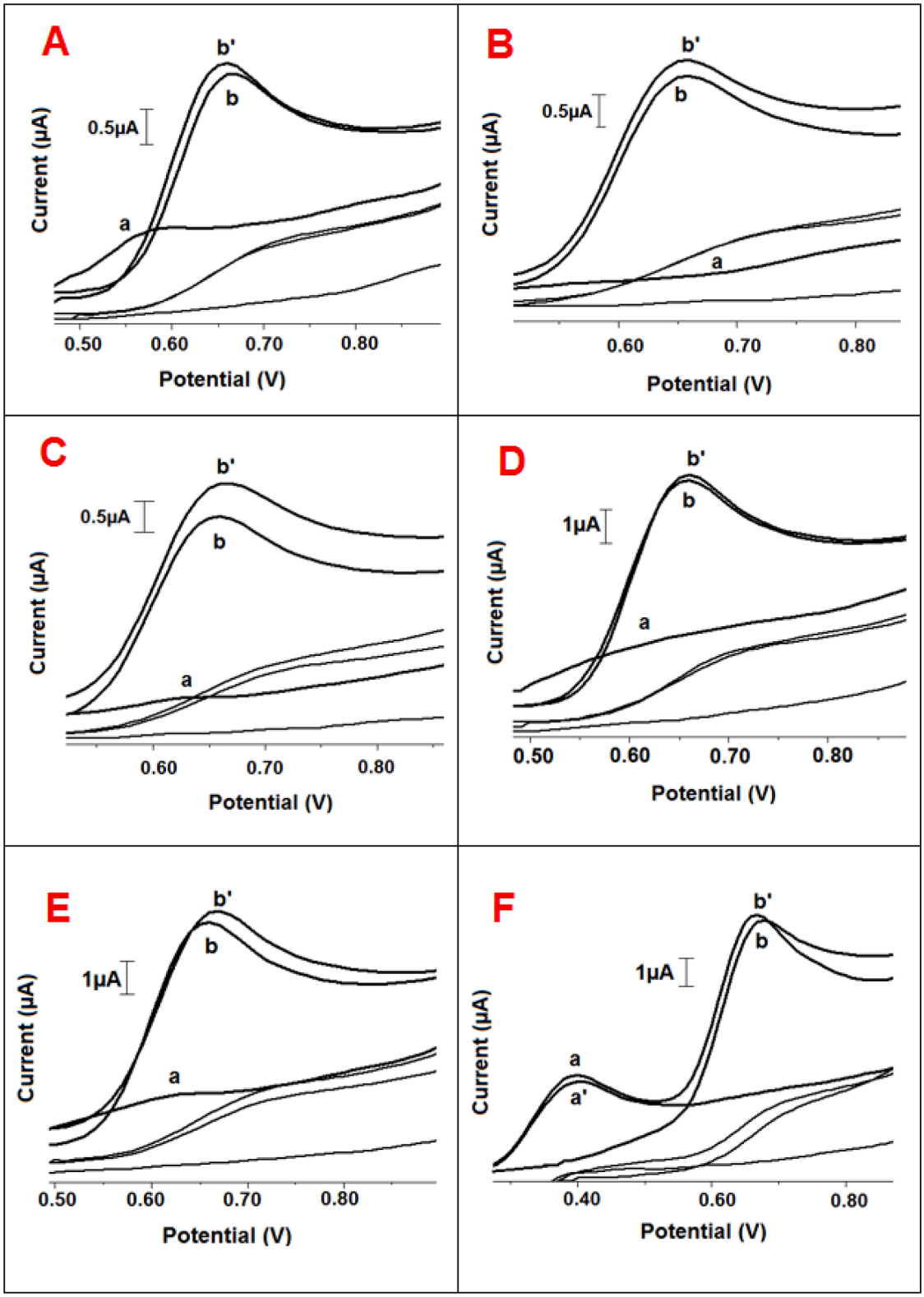

Fig. 6. Voltammograms of the oxidation signal of the interference factor **(a),** PNL signal **(b),** the signal of the interference factor **(a')** or PNL **(b')** in the presence of the mixture of 5 μg/mL PNL: 5μg/mL interference factor. The used interference factors are Cu^{2+} **(A),** Hg^{2+} **(B),** D(+) glucose **(C), 2,4-D (D),** m-PNL **(E)** or PRL **(F).**

mL PNL. The average PNL signals, control signals and recovery% values were given in Table 2. The recovery% values were in the acceptable ranges reported by Taverniers et al. [58]. These results showed that m-GMN/c-PGE based electrochemical sensor system could be applied for on-line monitoring of PNL and its derivatives in different water sources.

3.4. *Interference studies*

Voltammetric detection of PNL by using the m-GMN/c-PGEs in the

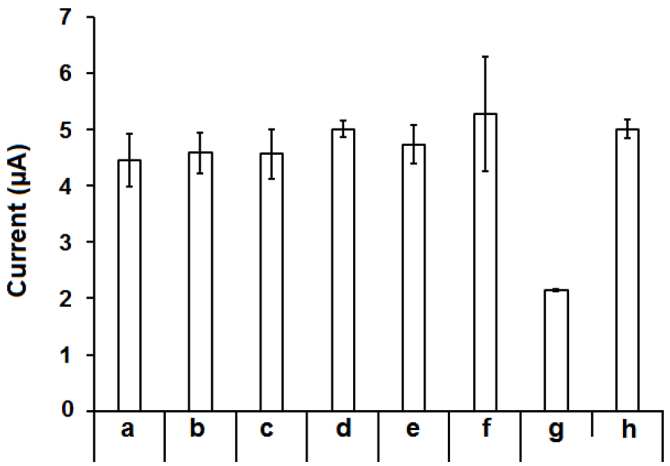

Fig. 7. Histograms representing the average signals measured at +0.66V in the presence of PNL **(a)** or the mixture of PNL:Cu^{2+} **(b),** PNL:Hg^{2+} **(c),** PNL:D(+) glucose **(d),** PNL:2,4-D **(e),** PNL:m-PNL **(f),** PNL: PRL **(h)** and the oxidation signal of PRL measured at +0.40 V **(g)** in the presence of the mixture of PNL: PRL ($n = 3$). All signals were measured in the presence of 5 μg/mL PNL or 5 μg/mL PNL: 5 μg/mL interference factor.

presence of the interference factors was investigated in the last part of the study. Results were given in Figs. 6 and 7. The average PNL signal in the presence of 5 μg/mL PNL was measured as 4.46 ± 0.47 μA with the RSD% as 10.46% ($n = 3$) (Fig. 7a). The average PNL signals in the presence of 5 μg/mL: 5 μg/mL Cu^{2+}, Hg^{2+}, D(+)glucose, 2,4-dichlorophenoxyacetic acid (2,4-D) and 2,6-di-tert-butyl-4-methylphenol (m-PNL) were found to be 4.58 ± 0.37 μA, 4.56 ± 0.44 μA, 5.07 ± 0.15 μA, 4.73 ± 0.34 μA and 5.27 ± 1.01 μA with the RSD% values as 8.06%, 9.69%, 2.94%, 7.20% and 19.22%, respectively (Fig. 7b to f). There were oxidation signals in the presence of 5 μg/mL of Cu^{2+}, Hg^{2+}, D(+) glucose, 2,4-D and m-PNL (Fig. S2 a to e) at +0.67 V but the signals were small and not reproducible. PNL detection was also investigated in the presence of worldwide used and phenol group containing drug, paracetamol (PRL). The oxidation signal of 5 μg/mL PRL was measured at +0.40 V (Fig. 6F-a) and the average PRL signal was found to be 1.99 ± 0.21 μA (RSD% = 10.47%, $n = 3$) (Fig. S2-f). In the presence of 5 μg/mL PNL:5 μg/mL PRL, the average PRL and PNL signals were measured as 2.15 ± 0.02 μA (Fig. 7g) and 5.00 ± 0.16 μA (Fig. 7h) (RSD% = 0.72% and 3.23% ($n = 3$), respectively). The recovery% values of the PNL signal in the presence of Cu^{2+}, Hg^{2+}, D(+)glucose, 2,4-D, m-PNL and PRL were calculated as 99.29%, 98.87%, 109.25%, 102.92%, 115.47% and 109.22%. These results indicated that the m-GMN/c-PGE based voltammetric sensor succesfully detected PNL in the presence of the interference factors.

3.5. Stability and repeatability of m-GMN/c-PGEs

The PNL signal was measured in the presence of 5μg/mL PNL by using freshly prepared m-GMN/c-PGEs (Fig. S3-a) or five days stored m-GMN/c-PGEs (Fig. S3-b) in order to study the stability of the m-GMN/c-PGEs. The average PNL signals were obtained as 4.46 ± 0.57 μA and 4.52 ± 0.66 μA with the RSD% values as 12.70% and 14.59% by using freshly prepared and five days stored m-GMN/c-PGEs, respectively. The detection of PNL was successfully achieved without signal loss even after five days preparation of m-GMN/c-PGEs.

For repeatability test, four different groups of m-GMN/c-PGEs were prepared ($n = 3$) and the measurement of 5 μg/mL PNL was performed (Fig. S4). The average PNL signals were measured as 4.76 ± 0.43 μA, 3.93 ± 0.21 μA, 3.98 ± 0.28 μA and 4.68 ± 0.12 μA with the RSD% values as 9.19%, 5.25%, 7.15% and 2.61%, respectively. The average PNL signal which was calculated based on the average PNL signals obtained in these four groups was found to be 4.33 ± 0.44 μA (RSD% = 10.16%, $n = 12$) which indicated that repeatable sensor response could be obtained by using m-GMN/c-PGEs.

4. Conclusion

Herein, chemical activation of disposable PGEs and m-GMN modification of the activated PGEs was successfully performed as the first time in the literature. The m-GMN/c-PGEs were applied for the voltammetric detection of PNL, sensitive and selective detection of PNL was achieved by using m-GMN/c-PGEs. The application of the sensor system in real samples was proven by monitoring of PNL in tap water, drinking water and industrial waste water samples. m-GMN was introduced into environmental monitoring area by combining the disposable electrochemical sensor technique within the scope of the present report. m-GMN/c-PGEs can be developed in a short time without requirement of complex experimental steps, however, further studies are needed to obtain miniaturized compact systems which are developed based on the fabrication procedure of m-GMN/c-PGEs. This study will lead to develop other m-GMN based electrochemical (bio)sensor systems for not only environmental applications but also biomedical studies including nucleic acid analysis, monitoring drug-DNA interactions, detection of proteins, etc .

CRediT authorship contribution statement

Gulsah Congur: Conceptualization, Methodology, Investigation, Writing – original draft, Writing – review & editing, Visualization.

Declaration of Competing Interest

The authors declare that they have no known competing financial interests or personal relationships that could have appeared to influence the work reported in this paper.

Acknowledgements

This study was partially supported from Bilecik Seyh Edebali University Scientific Research Project Coordination (Project number: 2020-01.BŞEÜ.12-02).

Supplementary materials

Supplementary material associated with this article can be found, in the online version, at doi:10.1016/j.surfin.2021.101268.

References

[1] A.K. Geim, K.S. Novoselov, The rise of graphene, Nat. Mater. 6 (2007) 183, https://doi.org/10.1038/nmat1849.
[2] A.K Geim, Graphene Prehistory, Phys. Scr. T146 (2012), 014003, https://doi.org/10.1088/0031-8949/2012/T146/014003.
[3] A.H. Castro Neto, F. Guinea, N.M.R. Peres, K.S. Novoselov, A.K. Geim, The electronic properties of graphene, Rev. Mod. Phys. 81 (2009) 109–162, https://doi.org/10.1103/RevModPhys.81.109.
[4] T. Hartman, J. Sturala, J. Luxa, Z. Sofe, Chemistry of germanene: surface modification of germanane using alkyl halides, ACS Nano 14 (2020) 7319–7327, https://doi.org/10.1021/acsnano.0c02635.
[5] B.N. Madhushankar, A. Kaverzin, T. Giousis, G. Potsi, D. Gournis, P. Rudolf, G. R. Blake, C.H. van Wal, B.J. Wees, Electronic properties of germanane field-effect transistors, 2D Mater. 4 (2017), 021009, https://doi.org/10.1088/2053-1583/aa57fd.
[6] N.G. Sahoo, R.J. Esteves, V.D. Punetha, D. Pestov, I.U. Arachchige, J.T. McLeskey, Schottky diodes from 2D germanane, Appl. Phys. Lett. 109 (2016), 023507, https://doi.org/10.1063/1.4955463.
[7] A.C. Serino, J.S. Ko, M.T. Yeung, J.J. Schwartz, C.B. Kang, S.H. Tolbert, R.B. Kaner, B.S. Dunn, P.S. Weiss, Lithium-ion insertion properties of solution-exfoliated germanane, ACS Nano 11 (2017) 7995, https://doi.org/10.1021/acsnano.7b02589.
[8] U. Srimathi, V. Nagarajan, R. Chandiramouli, Germanane nanosheet as a novel biosensor for liver cirrhosis based on adsorption of biomarker volatiles – A DFT study, Appl. Surf. Sci. 475 (2019) 990, https://doi.org/10.1016/j.apsusc.2019.01.008.

[9] U. Srimathi, V. Nagarajan, R. Chandiramouli, Detection of nucleobases using 2D germanane nanosheet: a first-principles study, Theor. Comput. Chem. 1130 (2018) 68, https://doi.org/10.1016/j.comptc.2018.03.011.

[10] S. Jiang, S. Butler, E. Bianco, O.D. Restrepo, W. Windl, J.E. Goldberger, Improving the stability and optical properties of germanane via one-step covalent methyl-termination, Nat. Commun. 5 (2014) 3389, https://doi.org/10.1038/ncomms4389.

[11] S. Jiang, K. Krymowski, T. Asel, M.Q. Arguilla, N.D. Cultrara, E. Yanchenko, X. Yang, L.J. Brillson, W. Windl, J.E. Goldberger, Tailoring the electronic structure of covalently functionalized germanane via the interplay of ligand strain and electronegativity, Chem. Mater. 28 (2016) 8071–8077, https://doi.org/10.1021/acs.chemmater.6b04309.

[12] Z. Liu, Z. Lou, Z. Li, G. Wang, Z. Wang, Y. Liu, B. Huang, S. Xia, X. Qin, X. Zhang, Y. Dai, GeH: a novel material as a visible-light driven photocatalyst for hydrogen evolution, Chem. Commun. 50 (2014) 11046–11048, https://doi.org/10.1039/C4CC03636K.

[13] H. Karimi-Maleh, Y. Orooji, F. Karimi, M. Alizadeh, M. Baghayeri, J. Rouhi, S. Tajik, H. Beitollahi, S. Agarwal, V.K. Gupta, S. Rajendran, A. Ayati, L. Fu, A. L. Sanati, B. Tanhaei, F. Sen, M. shabani-nooshabadi, P. Naderi Asrami, A. Al-Othman, A critical review on the use of potentiometric based biosensors for biomarkers detection, Biosens. Bioelectron. 184 (2021), 113252, https://doi.org/10.1016/j.bios.2021.113252.

[14] Y. Tian, L. Du, P. Zhu, Y. Chen, W. Chen, C. Wu, P. Wang, Recent progress in micro/nano biosensors for shellfish toxin detection, Biosens. Bioelectron. 176 (2021), 112899, https://doi.org/10.1016/j.bios.2020.112899.

[15] S. Takaloo, M.M. Zand, Wearable electrochemical flexible biosensors: With the focus on affinity biosensors, Sens. BioSensing Res. 32 (2021), 100403, https://doi.org/10.1016/j.sbsr.2021.100403.

[16] X. Zheng, F. Zhang, K. Wang, W. Zhang, Y. Li, Y. Sun, X. Sun, C. Li, B. Dong, L. Wang, L. Xu, Smart biosensors and intelligent devices for salivary biomarker detection, Trend Anal. Chem. 140 (2021), 116281, https://doi.org/10.1016/j.trac.2021.116281.

[17] H. Mahmoudi-Moghaddam, S. Tajik, H. Beitollahi, A new electrochemical DNA biosensor based on modified carbon paste electrode using graphene quantum dots and ionic liquid for determination of topotecan, Microchem. J. 150 (2019), 104085, https://doi.org/10.1016/j.microc.2019.104085.

[18] F.G. Nejad, S. Tajik, H. Beitollahi, I. Sheikhshoaie, Magnetic nanomaterials based electrochemical (bio)sensors for food analysis, Talanta 228 (2021), 122075, https://doi.org/10.1016/j.talanta.2020.122075.

[19] H. Beitollahi, H. Mahmoudi Moghaddam, S. Tajik, Voltammetric determination of bisphenol A in water and juice using a lanthanum (III)-doped cobalt (II,III) nanocube modified carbon screen-printed electrode, Anal. Letter 52 (2018) 1432–1444, https://doi.org/10.1080/00032719.2018.1545132.

[20] S. Bilal, M.M. Hassan, M. Fayyaz ur Rehman, M. Nasir, A.J. Sami, A. Hayat, An insect acetylcholinesterase biosensor utilizing WO_3/g-C_3N_4 nanocomposite modified pencil graphite electrode for phosmet detection in stored grains, Food Chem 346 (2021), 128894, https://doi.org/10.1016/j.foodchem.2020.128894.

[21] H. Zhao, X. Qiao, X. Zhang, C. Niu, T. Yue, Q. Sheng, Simultaneous electrochemical aptasensing of patulin and ochratoxin A in apple juice based on gold nanoparticlesdecorated black phosphorus nanomaterial, Anal. Bioanal. Chem. 413 (2021) 3131–3140, https://doi.org/10.1007/s00216-021-03253-3.

[22] L. Qian, S. Durairaj, S. Prins, A. Chen, Nanomaterial-based electrochemical sensors and biosensors for the detection of pharmaceutical compounds, Biosens. Bioelectron. 175 (2021), 112836, https://doi.org/10.1016/j.bios.2020.112836.

[23] Ž.Z. Tasić, M.B.P. Mihajlović, A.T. Simonović, M.B. Radovanović, M. M. Antonijević, Review of applied surface modifications of pencil graphite electrodes for paracetamol sensing, Results Phys. 22 (2021), 103911, https://doi.org/10.1016/j.rinp.2021.103911.

[24] G. Moro, F. Bottari, J.V. Loon, E.D. Bois, K.D. Wael, L.M. Moretto, Disposable electrodes from waste materials and renewable sources for (bio)electroanalytical applications, Biosens. Bioelectron. 146 (2019), 111758, https://doi.org/10.1016/j.bios.2019.111758.

[25] Y. Temerk, H. Ibrahim, W. Schuhmann, Simultaneous anodic adsorptive stripping voltammetric determination of luteolin and 3-hydroxyflavone in biological fluids using renewable pencil graphite electrodes, Electroanalysis 31 (2019) 1095–1103, https://doi.org/10.1002/elan.201900066.

[26] H. Ibrahim, Y. Temerk, A novel disposable electrochemical sensor based on modifying graphite pencil lead electrode surface with nanoacetylene black for simultaneous determination of antiandrogens flutamide and cyproterone acetate, J. Electroanal. Chem. 859 (2020), 113836 https://doi.org/10.1016/j.jelechem.2020.113836.

[27] Y.M. Temerk, H.S.M. Ibrahim, Individual and simultaneous square wave voltammetric determination of the anticancer drugs emodin and irinotecan at renewable pencil graphite electrodes, J. Braz. Chem. Soc. 24 (2013) 1669–1678, https://doi.org/10.5935/0103-5053.20130214.

[28] I.G. David, D.-E. Popa, M. Buleandra, Pencil graphite electrodes: a versatile tool in electroanalysis, J. Anal. Methods Chem. 2017 (2017) 1–22, https://doi.org/10.1155/2017/1905968.

[29] Á. Torrinha, C.G. Amorim, M.C.B.S.M. Montenegro, A.N. Araújo, Biosensing based on pencil graphite electrodes, Talanta 190 (2018) 235–247, https://doi.org/10.1016/j.talanta.2018.07.086.

[30] M. Santhiago, L.T. Kubota, A new approach for paper-based analytical devices with electrochemical detection based on graphite pencil electrodes, Sens. Act. B 177 (2013) 224, https://doi.org/10.1016/j.snb.2012.11.002.

[31] E.N.T Silva, V.S. Ferreira, B.G. Lucca, Rapid and inexpensive method for the simple fabrication of PDMS-based electrochemical sensors for detection in microfluidic devices, Electrophoresis 40 (2019) 1322–1330, https://doi.org/10.1002/elps.201800478.

[32] Y. Huang, X. Hu, H. Zhao, D. He, Y. Li, M. Yang, Z. Yu, K. Li, J. Zhang, Composite alkali polysaccharide supramolecular nanovesicles improve biocharacteristics and anti-lung cancer activity of natural phenolic drugs via oral administration, Int. J. Pharm. 573 (2020), 118864, https://doi.org/10.1016/j.ijpharm.2019.118864.

[33] H. Denghel, T. Göen, Simultaneous assessment of phenolic metabolites in human urine for a specific biomonitoring of exposure to organophosphate and carbamate pesticides, Toxicol Lett 298 (2018) 33–41, https://doi.org/10.1016/j.toxlet.2018.07.048.

[34] W. Nabgan, B. Nabgan, T.A.T. Abdullah, N. Ngadi, A.A. Jalil, N.S. Hassan, S. MaryamIzan, W.S. Luing, S.N. Abdullah, F.S.A. Majee, Conversion of polyethylene terephthalate plastic waste and phenol steam reforming to hydrogen and valuable liquid fuel: synthesis effect of Ni–Co/ZrO_2 nanostructured catalysts, Int. J. Hydrog. Energy 45 (2020) 6302–6317, https://doi.org/10.1016/j.ijhydene.2019.12.103.

[35] E.S.Z. El-Ashtoukhy, Y.A. El-Taweel, O. Abdelwahab, E.M. Nassef, Treatment of petrochemical wastewater containing phenolic compounds by electrocoagulation using a fixed bed electrochemical reactor, Int. J. Electrochem. Sci. 8 (2013) 1534–1550.

[36] M.A. Fawzy, S. Alharthi, Cellular responses and phenol bioremoval by green alga Scenedesmus abundans: Equilibrium, kinetic and thermodynamic studies, Environ. Technol. Innov. 22 (2021), 101463, https://doi.org/10.1016/j.eti.2021.101463.

[37] Z. Bo, T. Zhibo, Synthesis of Au nanoparticles decorated carbon nanotubes as an electrochemical sensor for phenol determination in petrochemical wastewater, Int. J. Electrochem. Sci. 15 (2020) 6177–6187, https://doi.org/10.20964/2020.07.03.

[38] K.Y. Hwa, A. Ganguly, S.K.S. Tata, Influence of temperature variation on spinel-structure MgFe2O4 anchored on reduced graphene oxide for electrochemical detection of 4-cyanophenol, Microchim. Acta 187 (2020) 633, https://doi.org/10.1007/s00604-020-04613-z.

[39] D. Wibowo, Y. Sufandy, T.Azis I.Irwan, M. Maulidiyah, M. Nurdin, Investigation of nickel slag waste as a modifier on graphene-TiO_2 microstructure for sensing phenolic compound, J. Mater. Sci. Mater. Electron. 31 (2020) 14375–14383, https://doi.org/10.1007/s10854-020-03996-2.

[40] S. Guo, J. Raya, D. Ji, Y. Nishina, C. Ménard-Moyon, A. Bianco, s carboxylation an efficient method for graphene oxide functionalization? Nanoscale Adv 2 (2020) 4085–4092, https://doi.org/10.1039/D0NA00561D.

[41] P. Qian, S. Ai, H. Yin, J. Li, Evaluation of DNA damage and antioxidant capacity of sericin by a DNA electrochemical biosensor based on dendrimer-encapsulated Au-Pd/chitosan composite, Microchim. Acta 168 (2010) 347, https://doi.org/10.1007/s00604-009-0280-x.

[42] Z. Liu, Z. Wang, Q. Sun, Y. Dai, B. Huang, Methyl-terminated germanane $GeCH_3$ synthesized by solvothermal method with improved photocatalytic properties, App. Surf. Sci. 881 (2019) 467–468, https://doi.org/10.1016/j.apsusc.2018.10.228.

[43] N.F. Rosli, N. Nohaizad, J. Sturala, A.C. Fisher, R.C. Webster, M. Pumera, Siloxene, germanane, and methylgermanane: functionalized 2D materials of group 14 for electrochemical applications, Adv. Funct. Mater. 30 (2020), 1910186, https://doi.org/10.1002/adfm.201910186.

[44] T.E. Cummings, P.J. Elving, Determination of the electrochemically effective electrode area, Anal. Chem. 50 (1978) 480, https://doi.org/10.1021/ac50025a031.

[45] B. Habibi, S. Pashazadeh, L.A. Saghatforoush, A. Pashazadeh, Direct electrochemical synthesis of the copper based metal-organic framework on/in the heteroatoms doped graphene/pencil graphite electrode: highly sensitive and selective electrochemical sensor for sertraline hydrochloride, J. Electroanal. Chem. 888 (2021), 115210, https://doi.org/10.1016/j.jelechem.2021.115210.

[46] M. Wen, H. Liu, F. Zhang, Y. Zhu, D. Liu, Y. Tian, Q. Wu, Amorphous FeNiPt nanoparticles with tunable length for electrocatalysis and electrochemical determination of thiols, Chem. Commun. (2009) 4530–4532, https://doi.org/10.1039/b907379e.

[47] E.Eksin Isin, A. Erdem, Graphene oxide modified single-use electrodes and their application for voltammetric miRNA analysis, Mater. Sci. Eng. C 75 (2017) 1242–1249, https://doi.org/10.1016/j.msec.2017.02.166.

[48] J.N. Miller, J.C. Miller, Statistics and Chemometrics for Analytical Chemistry, 6th ed., Pearson Education, Essex, 2005.

[49] L. Wang, Y. Liu, R. Yang, J. Li, L. Qu, AgNPs–PDA–GR nanocomposites-based molecularly imprinted electrochemical sensor for highly recognition of 2,4,6-trichlorophenol, Microchem. J. 159 (2020), 105567, https://doi.org/10.1016/j.microc.2020.105567.

[50] Y. Zhang, Q. Xie, Z. Xia, G. Gui, F. Deng, Fulvic acid reduced GO and phthalocyanine nanorods as reaction platform for simultaneous determination of catechol, hydroquinone, phenol and p-nitrophenol, J. Electrochem. Soc. 166 (2019) B1293–B1299, https://doi.org/10.1149/2.0351914jes.

[51] G. Zhu, Qian Tang, Jinlei Dou, Xuan Li, Jianmao Yang, Ran Xu, Jianyun Liu, The Electrochemical society, partially reduced graphene oxide sheet-covered polyaniline nanotubes for the simultaneous determination of bisphenol a and phenol, J. Electrochem. Soc. 166 (2019) B1661–B1668, https://doi.org/10.1149/2.1381915jes.

[52] Y. Su, X. Zheng, H. Cheng, M. Rao, K. Chen, J. Xi, L. Lin, H. Zhu, Mn-Fe_3O_4 nanoparticles anchored on the urushiol functionalized 3D-graphene for the electrochemical detection of 4-nitrophenol, J. Hazard Mater. 409 (2021), 124926, https://doi.org/10.1016/j.jhazmat.2020.124926.

[53] R. Nissim, R.G. Compton, Introducing absorptive stripping voltammetry: wide concentration range voltammetric phenol detection, Analyst 139 (2014) 5911, https://doi.org/10.1039/c4an01417k.

[54] A.V. Kolliopoulos, D.K. Kampouris, C.E. Banks, Indirect electroanalytical detection of phenols, Analyst 140 (2015) 3244, https://doi.org/10.1039/c4an02374a.
[55] Y. Wen, R. Li, J. Liu, X. Zhang, P. Wang, X. Zhang, B. Zhou, H. Li, J. Wang, Z. Li, B. Sun, Promotion effect of Zn on 2D bimetallic NiZn metal organic framework nanosheets for tyrosinase immobilization and ultrasensitive detection of phenol, Anal. Chim. Acta 1127 (2020) 131–139, https://doi.org/10.1016/j.aca.2020.06.062.
[56] B.T.P. Quynh, J.Y. Byun, S.H. Kim, Non-enzymatic amperometric detection of phenol and catechol using nanoporous gold, Sens. Act. B 221 (2015) 191–200, https://doi.org/10.1016/j.snb.2015.06.067.
[57] M. Rachna, U. Rani, J. Shanker, Sunlight assisted degradation of toxic phenols by zinc oxide doped prussian blue nanocomposite, Environ. Chem. Eng. 8 (2020), 104040, https://doi.org/10.1016/j.jece.2020.104040.
[58] I. Taverniers, M. Loose, E.V. Bockstaele, Trends in quality in the analytical laboratory. II. Analytical method validation and quality assurance, Trend. Anal. Chem. 23 (2004) 535–552, https://doi.org/10.1016/j.trac.2004.04.001.